Improvement Performances of Sensorless Control for PMSM Based on FOC Strategy Using Luenberger Observer, Sine Cosine Algorithm, and RL-TD3 Agent

Marcel Nicola
Research Department
National Institute for Research, Development and Testing in Electrical Engineering – ICMET Craiova
Department of Automatic Control and Electronics
University of Craiova
Craiova, Romania
marcel_nicola@icmet.ro, marcel_nicola@edu.ucv.ro

Claudiu-Ionel Nicola
Research Department
National Institute for Research, Development and Testing in Electrical Engineering – ICMET Craiova
Department of Automatic Control and Electronics
University of Craiova
Craiova, Romania
nicolaclaudiu@icmet.ro, claudiu_nicola@edu.ucv.ro

2023 International Conference on Electromechanical and Energy Systems (SIELMEN) | 979-8-3503-1524-0/23/$31.00 ©2023 IEEE | DOI: 10.1109/SIELMEN59038.2023.10290813

***Abstract*—Considering the need to increase the reliability of Permanent Magnet Synchronous Motor (PMSM) control systems by eliminating speed sensors and using observers to estimate PMSM rotor speed, this paper shows a sensorless control structure-type based on the Field Oriented Control (FOC) type strategy and a Luenberger observer. In order to achieve a better performance of the observer in terms of reducing the error given by the difference between the measured value of the PMSM rotor speed and the Luenberger observer output, a Sine Cosine Algorithm (SCA) is used to optimize the tuning parameters of the Luenberger observer. Also, in order to increase the Luenberger observer performance, a Reinforcement Learning (RL), namely Twin-Delayed Deep Deterministic Policy Gradient (TD3) agent is used, which after the training process supply a signal that is added to the Luenberger observer output, thus obtaining superior features of the estimation for PMSM speed. These methods to improve Luenberger observer performance are validated by numerical simulations realized in Matlab/Simulink.**

Keywords—PMSM, Luenberger, SCA algorithm, reinforcement learning.

I. INTRODUCTION

One option for increasing the overall reliability of a control system for PMSM-type motor is the use of rotor speed observers. They provide instantaneous speed estimation by eliminating motion sensors from the conventional speed transducer component. Given that the concern for the study of PMSM and its use in a number of industrial applications and more is growing in the last decade, and hence the interest in finding ways to increase reliability and ways to estimate PMSM rotor speed is evident [1-5]. From the point of view of PMSM control, FOC [6, 7] and Direct Torque Control (DTC) [8, 9] strategies can be recalled. Among the specific control algorithms it can be said that there is a wide range of PMSM control algorithms, from which optimal PMSM control structures can be chosen according to performance/cost criteria. Among the usual control algorithms it can be mentioned: adaptive algorithms [10], predictive algorithms [11], robust algorithms [12], neuro-fuzzy algorithms [13], etc.

This paper was elaborated as part of the "NUCLEU Program within the framework of the National Research, Development and Innovation Plan for 2022-2027, developed with the support of Ministry of Research, Innovation and Digitization, Project No PN 23 33 02 04".

Among the usual observers used for estimating PMSM rotor speed are: SMO [14], MRAS [15], ESO [16], and DO [17] for the deterministic case, but also Kalman observer for the stochastic case [18]. A particular observer is the Luenberger observer [19] as it is one of the first observers used for estimating various signals in control systems, but it has a relatively low complexity structure with good estimation performance, which recommends the Luenberger observer for both design study and real time implementation. Thus, in this paper it is presented a PMSM velocity estimation using a Luenberger observer along with two ways to improve the estimation performance by means of an SCA-type algorithm and [20] an RL TD3 agent [21, 22].

The rest of the paper is structured as follows: Section II shows the proposed PMSM sensorless control system based on Luenberger observer, and Section III presents the improvement of the Luenberger observer performances. The Matlab/Simulink implementation of the proposed PMSM sensorless control system and numerical simulations are presented in Section IV. The last part shows some conclusions and a few ideas for next works.

II. PROPOSED SENSORLESS CONTROL SYSTEM OF PMSM BASED ON LUENBERGER OBSERVER

Starting from the FOC-type control structure, when using a sensorless control system based on the Luenberger observer, this paper proposes to improve the estimation of the PMSM speed and PMSM rotor position. Ways to improve the sensorless control structure consist on the one hand in optimizing the tuning parameters of the observer, and on the other hand in using a type of RL agent, which provides superior estimation performance by bringing the estimated speed signal closer to the measured speed signal, following the training and design phase. The schematic diagram of the sensorless control structure using the Luenberger observer together with the ways to improve it proposed in this paper is shown in Figure 1. The functioning equations of a PMSM described in the *d-q* frame system are given in equation (1). In this equation is used the following notations: u_d, u_q, i_d, i_q, R_d, R_q, L_d, L_q – voltages, currents resistances, and inductances on *d-q* axes; ω – rotor speed; θ_e – rotor electrical angle; B – coefficient of viscous friction; J – the PMSM rotor and load

979-8-3503-1524-0/23/$31.00 ©2023 IEEE

inertia; λ_0 – permanent magnet flux linkage; n_p – pole pairs number; T_L – load torque. It also accepts the following usual simplification namely: $L_d = L_q = L$; $R_d = R_q = R_s$.

$$\begin{cases} \dfrac{di_d}{dt} = -\dfrac{R_s}{L_d} i_d + \dfrac{L_q}{L_d} n_p \omega i_q + \dfrac{1}{L_d} u_d \\ \dfrac{di_q}{dt} = -\dfrac{R_s}{L_q} i_q - \dfrac{L_d}{L_q} n_p \omega i_d - \dfrac{\lambda_0}{L_q} n_p \omega + \dfrac{1}{L_q} u_q \\ \dfrac{d\omega}{dt} = \dfrac{3n_p}{2J}\left(\lambda_0 i_q + \left(L_d - L_q\right) i_d i_q\right) - \dfrac{1}{J} T_L - \dfrac{B}{J}\omega \\ \dfrac{d\theta_e}{dt} = n_p \omega \end{cases} \quad (1)$$

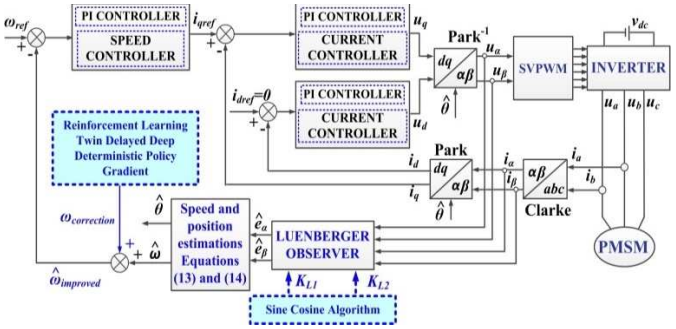

Fig. 1. Proposed architecture of the PMSM sensorless control using Luenberger-type observer.

III. Improvement of the Luenberger Observer Performaces

This section presents the structure of a Luenberger-type observer together with two ways to improve this observer, namely to estimate as accurately as possible the PMSM velocity in relation to the measured velocity. The two methods are briefly described below. Thus, the first method consists in optimizing the tuning parameters of the Luenberger observer using an SCA algorithm. The second method of improving the performance of the Luenberger-type observer is to use a specially trained RL TD3 agent to provide the necessary corrections which when added to the observer output provide a more accurate estimate of the speed relative to the measured speed. The schematic diagram of the Luenberger-type observer is depicted in Figure 2.

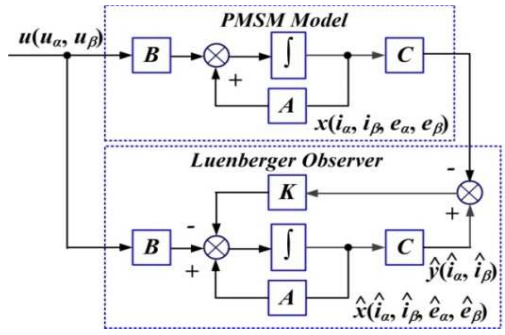

Fig. 2. Block schemtic of the Luenberger observer.

A. Mathematical Description of the Luenberger Observer

The PMSM voltage equations in *abc* three-phase frame are the following:

$$\begin{cases} u_a = i_a R_s + \dfrac{d\lambda_a}{dt} \\ u_b = i_b R_s + \dfrac{d\lambda_b}{dt} \\ u_c = i_c R_s + \dfrac{d\lambda_c}{dt} \end{cases} \quad (2)$$

where: λ_a, λ_b, and λ_c represents the three-phase flux linkage corresponding on *abc* frame stator winding and can be expressed as follows:

$$\begin{cases} \lambda_a = Li_a + \lambda_0 \\ \lambda_b = Li_b + \lambda_0 \\ \lambda_c = Li_c + \lambda_0 \end{cases} \quad (3)$$

To obtain the Luenberger-type observer equations, Clarke and Park transformations are used to obtain the description of the PMSM operating equations in α-β frame, as in the relations:

$$\begin{cases} L\dfrac{di_\alpha}{dt} = u_\alpha - e_\alpha - Ri_\alpha \\ L\dfrac{di_\beta}{dt} = u_\beta - e_\beta - Ri_\beta \end{cases} \quad (4)$$

where: e_α and e_β represents the back-EMF of PMSM and are expressed in equation (5) [5].

$$\begin{cases} e_\alpha = -\lambda_0 \omega \sin\theta \\ e_\alpha = \lambda_0 \omega \cos\theta \end{cases} \quad (5)$$

The voltage equations expressed in *d*-*q* frame are given in the next form:

$$\begin{cases} u_d = Ri_d + \dfrac{d\lambda_d}{dt} - \lambda_q \omega \\ u_q = Ri_q + \dfrac{d\lambda_q}{dt} - \lambda_d \omega \end{cases} \quad (6)$$

The PMSM stator flux linkages component on *d*-axis and *q*-axis from equation (6) can be expressed as in the following equation:

$$\begin{cases} \lambda_d = \lambda_0 + L_d i_d \\ \lambda_q = L_q i_q \end{cases} \quad (7)$$

Also, the equation expression of the electromagnetic PMSM T_e is given below:

$$T_e = \frac{3}{2}\frac{n_p}{J}\left(\lambda_0 i_q + \left(L_d - L_q\right) i_d i_q\right) \tag{8}$$

Note that for $i_d = 0$, the maximum electromagnetic torque T_e is obtained.

In Figure 2 it is noted with i_α, i_β stator currents and u_α, u_β voltages in the α-β frame. Thus, the state vector is defined as $x = \begin{bmatrix} i_\alpha & i_\beta & e_\alpha & e_\beta \end{bmatrix}^T$, input vector as $u = \begin{bmatrix} u_\alpha & u_\beta \end{bmatrix}^T$, and output vector as $y = \begin{bmatrix} i_\alpha & i_\beta \end{bmatrix}^T$.

$\hat{e}_\alpha$ and $\hat{e}_\beta$ are the estimated values of back-EMF e_α and e_β.

Starting from the standard form of the initial system given in equation (9), the Luenberger-type observer is given in equation (10), and by customizing the component vectors, the form of equation (11) is obtained.

Further, it is defined the relations (12) where K_{L1} and K_{L2} are the amplifications of the Luenberger observer and represent its tuning parameters.

$$\begin{cases} \dot{x} = \boldsymbol{A}x + \boldsymbol{B}u \\ y = \boldsymbol{C}x \end{cases} \tag{9}$$

$$\begin{cases} \dot{\hat{x}} = \boldsymbol{A}\hat{x} + \boldsymbol{B}u - \boldsymbol{K}(y - \hat{y}) \\ \hat{y} = \boldsymbol{C}\hat{x} \end{cases} \tag{10}$$

$$\begin{cases} L\dfrac{d\hat{i}_\alpha}{dt} = u_\alpha - \hat{e}_\alpha - Ri_\alpha + K_{L1}(i_\alpha - \hat{i}_\alpha) \\ L\dfrac{d\hat{i}_\beta}{dt} = u_\beta - \hat{e}_\beta - Ri_\beta + K_{L1}(i_\beta - \hat{i}_\beta) \end{cases} \tag{11}$$

where:

$$\begin{aligned} \hat{e}_\alpha &= -K_{L2}(i_\alpha - \hat{i}_\alpha) \\ \hat{e}_\beta &= -K_{L2}(i_\beta - \hat{i}_\beta) \end{aligned} \tag{12}$$

With these the estimates of the PMSM rotor position and the velocity of the PMSM can be defined in equations (13) and (14), in this case the associated electrical quantities.

In the usual implementation in addition to the equations showing the operation of the Luenberger observer, low-pass filters are also used to increase the accuracy of the estimation.

$$\hat{\theta}_e = \arctan\left(-\frac{\hat{e}_\alpha}{\hat{e}_\beta}\right) \tag{13}$$

$$\hat{\omega}(t) = \frac{\sqrt{\hat{e}_\alpha^2 + \hat{e}_\beta^2}}{\lambda_0} \tag{14}$$

B. Sine Cosine Algorithm

This type of optimization algorithm is meta-heuristic. After generating the initial solutions from the search space, based on the input sizes, the next solutions are generated at each iteration by minimizing an optimization criterion. Particularly compared to other meta-heuristic optimization algorithms, this algorithm generates the way in which the new solutions are obtained based on the fact that the sine and cosine functions are harmonic. In the case of the Luenberger observer described above, the SCA-type algorithm is used to optimize the K_{L1} and K_{L2} tuning parameters. The proposed objective function is the integral of the square of the error signal between the measured rotor velocity and the estimated rotor velocity using the Luenberger observer. Obviously the integral of the objective function, in the implementation is transformed into a discrete sum which is iteratively minimized in the SCA-type algorithm.

C. RL TD3 agent

Another way to achieve superior features of PMSM velocity estimation with the Luenberger observer is to drive and insert in tandem with this observer an RL TD3 agent. During training, the RL TD3 agent iteratively tries to maximize the reward given in equation (15).

After the RL TD3 agent is trained and operates in tandem with the Luenberger observer, it will supply signals that superimposed with the observer's estimate will result in a PMSM velocity estimation as close as possible with the measured PMSM velocity.

$$r_{Luenberger} = -\left(5\omega_{err}^2 + 0.1\sum_j \left(u_{t-1}^j\right)^2\right) \tag{15}$$

where: u_{t-1}^j is the action value from previous iteration.

IV. MATLAB/SIMULINK IMPLEMENTATION AND NUMERICAL SIMULATIONS

The following presents the Matlab/Simulink implementation of the structure of a PMSM implying a Luenberger observer and an associated RL TD3 agent as described in Section III. The nominal values of the PMSM's parameters used in realized numerical simulations are summarized in Figure 3.

Parameter	Value	Unit
PMSM stator resistance: R_s	2.875	Ω
PMSM inductances: L_d and L_q	0.0085	H
PMSM rotor moment of inertia: J	8e-3	kg·m²
PMSM viscous friction: B	0.01	N·m·s/rad
PMSM flux linkage: λ_0	0.175	WB
Pole pairs number: n_p	4	–

Fig. 3. Values of the PMSM nominal parameters for numerical simulations.

Figure 4 shows the Matlab/Simulink implementation for the case liked sensored or sensorless control system of a PMSM using the FOC strategy. For the estimation of the PMSM rotor velocity, both the use of a Luenberger observer and the improved variants for the estimation of the velocity in relation to the measured speed by means of an SCA-type algorithm and an RL TD3 agent are shown in comparison. Also, Figure 5 shows by using of the operating equations described in Section III the implementation of the Matlab/Simulink subsystem diagram model of the Luenberger observer. Figure 6 shows the Matlab/Simulink model subsystem implementation diagram of the RL TD3 agent for increasing the performance of Luenberger observer PMSM velocity estimation. Figure 7 shows the run-time performance of the SCA algorithm for the optimization of the gain parameters K_{L1} and K_{L2} of the Luenberger observer. Thus, in Figure 7 it can be seen that after the required 100 iterations, the best cost indicator has a convergent evolution thus indicating that the training of the SCA algorithm was successful. The training features of the RL TD3 algorithm for improving the Luenberger observer is presented in Figure 8.

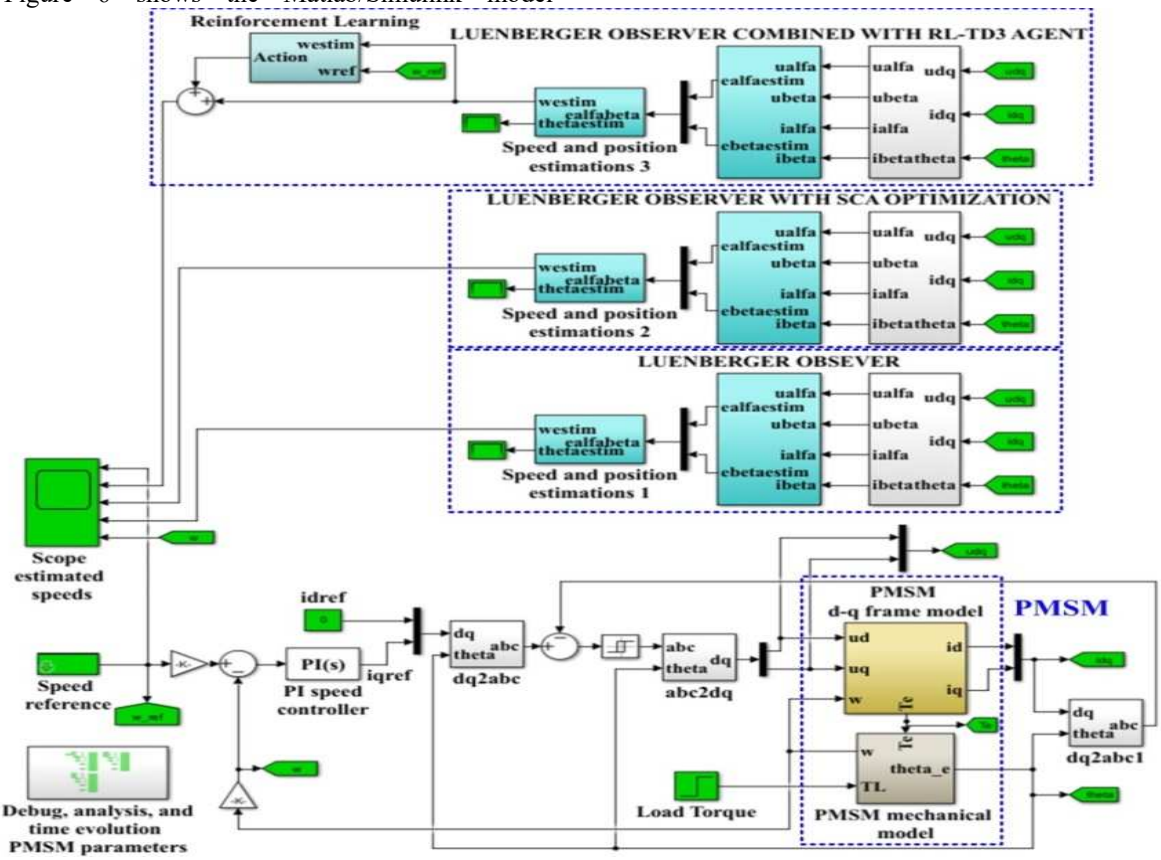

Fig. 4. Simulink model of the sensorless control system of PMSM based on improved Luenberger-type observer using SCA-type algorithm and RL TD3-type agent.

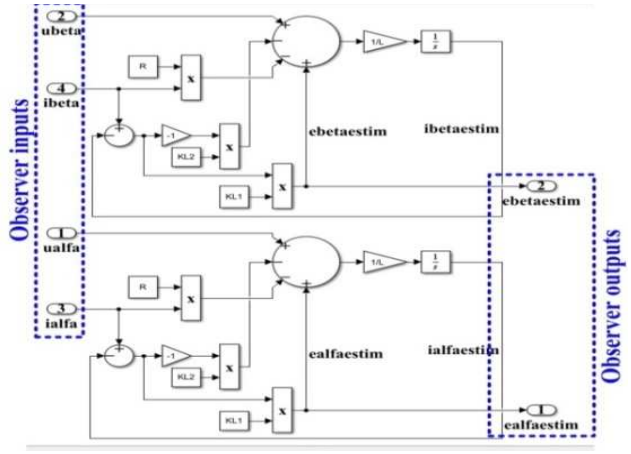

Fig. 5. Matlab/Simulink subsystem model implementation of the Luenberger observer.

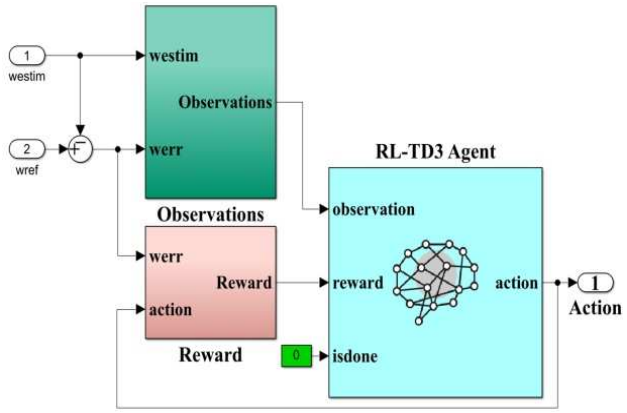

Fig. 6. Matlab/Simulink subsystem model diagram implementation of the RL TD3 agent for improvement of Luenberger observer PMSM velocity estimation.

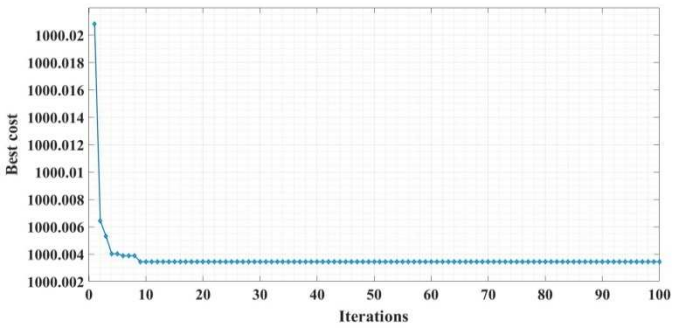

Fig. 7. Training performance of the SCA-type algorithm for tuning gain parameters of the Luenberger observer.

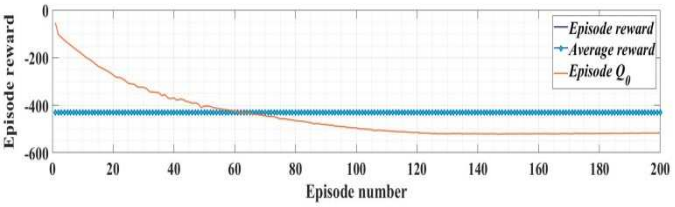

Fig. 8. Training performance of the RL TD3 algorithm for improvement of Luenberger observer.

Further, it is pointed out that the optimal values for the tuning parameters K_{L1} and K_{L2} used in the structure of the Luenberger observer are the following: K_{L1} = 205 and K_{L2} = 1.059.

The numerical simulations realized in Matlab/Simulink environment and shown in Figure 9, 10, and 11 represents the time evolution of the main sizes of interest, namely: PMSM measured rotor velocity and estimated PMSM rotor speed, electromagnetic - torque T_e and load - torque T_L, stator currents i_a, i_b, i_c, and current i_d from d-axis and current i_q from q-axis.

These constitute the response to step signals of the reference speed ω_{ref} under the FOC-type control structure and the PMSM rotor velocity is both measured and estimated using a Luenberger observer along with the performance improvement variants presented in Section III.

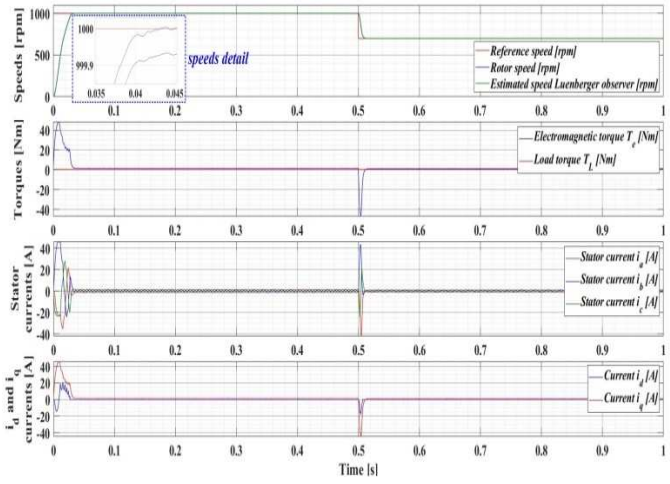

Fig. 9. Comparative time evolution between the PMSM measured rotor velocity and the estimated PMSM rotor velocity using Luenberger observer basic version.

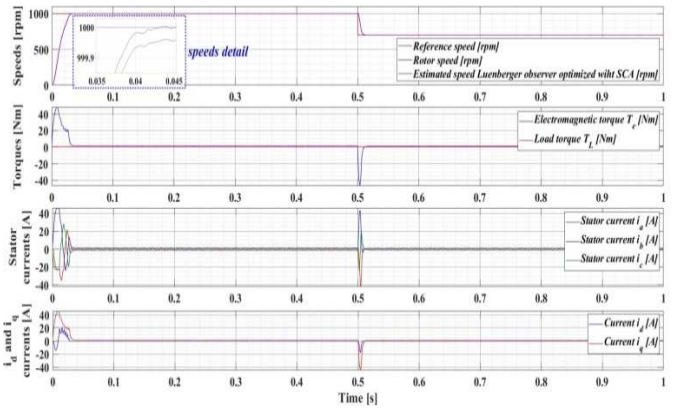

Fig. 10. Comparative time evolution between the PMSM measured rotor velocity and the estimated PMSM rotor velocity using Luenberger observer optimized with SCA-type algorithm.

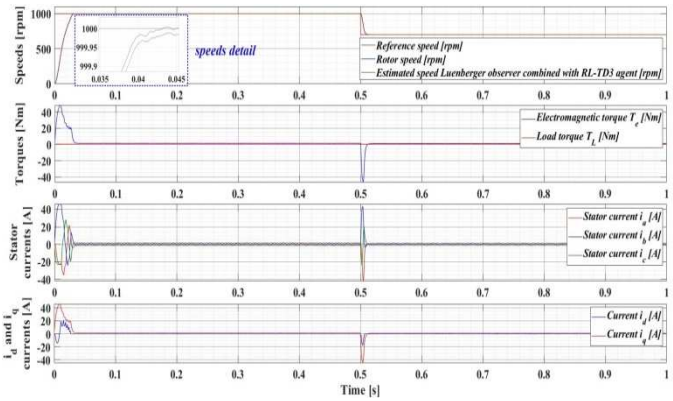

Fig. 11. Comparative evolution between the PMSM measured rotor velocity and the estimated PMSM rotor speed using Luenberger observer combined with RL TD3 agent.

The comparative time evolution between the measured rotor velocity of the PMSM and the estimated rotor velocity of the PMSM using the basic version of the Luenberger observer, the Luenberger observer optimized with the SCA algorithm and the Luenberger observer combined with the RL TD3-type agent is shown in Figure 12. Also, Figure 13 shows the comparative evolution of the PMSM rotor position, both in the version where the PMSM rotor position is measured and in the version where the PMSM rotor position is estimated using a Luneberger-type observer.

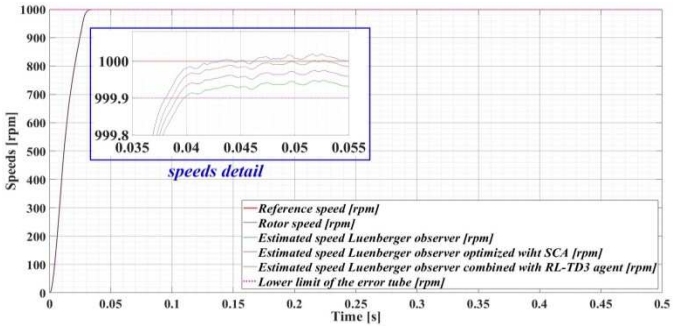

Fig. 12. Comparative time evolution between the PMSM measured rotor velocity and the estimated PMSM rotor velocity using Luenberger observer basic version, Luenberger observer optimized with SCA-type algorithm, and Luenberger observer combined with RL TD3-type agent.

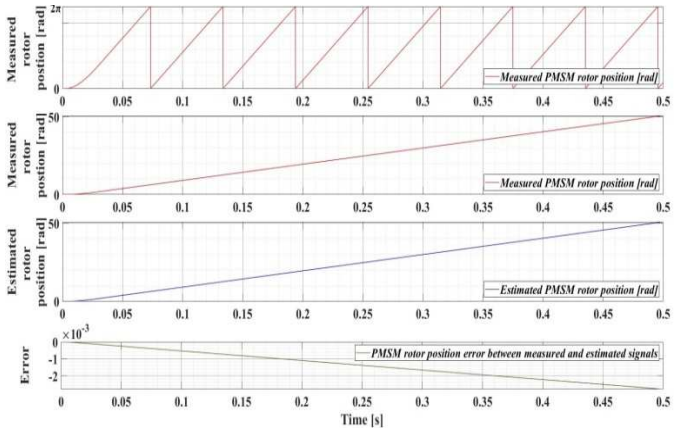

Fig. 13. Time evolution for measured PMSM rotor position and estimated PMSM rotor position.

Table I summarizes the comparative performance of PMSM rotor velocity estimation, both when using the Luenberger observer basic version and when improving the performance of PMSM rotor velocity estimation using the SCA-type algorithm and the respective RL TD3 agent.

An improvement of the Luenberger observer basic version performance is observed both in terms of response time and rotor speed ripple, using the performance improvement methods presented above. Clearly, due to the structure and operation of the RL TD3-type agent in tandem with a Luenberger observer basic version, a 2.77% improvement in response time and a 5.84% improvement in speed ripple are achieved.

TABLE I. PERFORMANCES OF THE IMPROVED LUENBERGER OBSERVER.

Luenberger Observer	Response time [s]	Response time improvement with Luenberger observer basic version [%]	Rotor speed ripple [rpm]	Rotor speed ripple improvement with Luenberger observer basic version [%]
Basic version	0.0397	–	3.168	–
Basic version with optimized parameters using SCA-type algorithm	0.0392	1.26	3.087	2.56
Basic version combined with RL TD3 agent	0.0386	2.77	2.983	5.84

When testing the parametric robustness of the Luenberger observer on the PMSM velocity estimation, Figure 14 shows the comparative time evolution between the measured PMSM rotor speed and the estimated PMSM velocity using the Luenberger observer combined with the RL TD3-type agent with the *J* parameter increased by 100%. It is observed that the Luenberger observer provides good results also in this case in terms of the error seen in the dynamic and steady state regime, with a normal increase in response time.

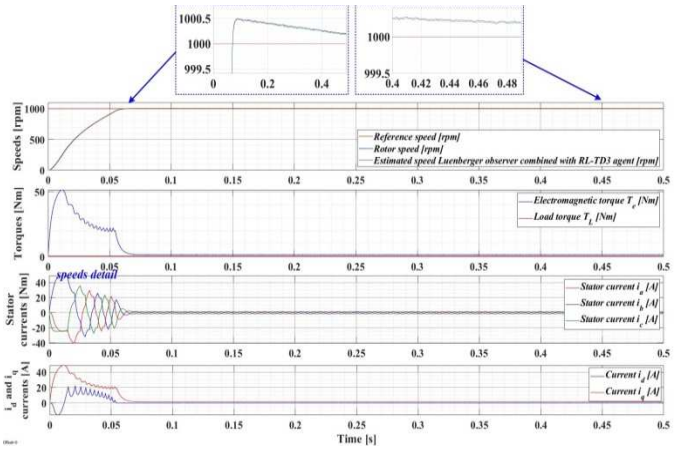

Fig. 14. Comparative time evolution between the PMSM measured rotor velocity and the estimated PMSM rotor velocity using Luenberger observer combined with RL TD3 agent with *J* parameter increased with 100%.

V. CONCLUSIONS

In this paper it is presented a way to estimate the PMSM rotor velocity using Luenberger observer. The control strategy of the PMSM is FOC and the equations of operation, algorithms and implementation in Matlab/Simulink are presented.

As methods to enhance the PMSM rotor velocity estimates using Luenberger observer compared to PMSM measured rotor speed two ways are presented, namely: optimization of the Luenberger observer tuning parameters and use of a RL TD3 agent. Following numerical simulations, the improvements brought by the two presented methods are presented.

In future work, improved variants of the Luenberger observer structure will be presented using other tuning parameter optimization algorithms.

REFERENCES

[1] S. Zossak, M. Musak, M. Stulrajter, P. Makys, "Challenges of Sensorless Controlled High-speed PMSM Drives," *IEEE 10th International Symposium on Sensorless Control for Electrical Drives (SLED)*, Turin, Italy, 2019, pp. 1-6.

[2] P. Maity, "Observer-based Sensorless Field oriented control of PMSM motor for EV application," *International Conference on Recent Trends on Electronics, Information, Communication & Technology (RTEICT)*, Bangalore, India, 2021, pp. 274-279.

[3] Z. Chen, C. Xiao, X. Zhang, C. Liu, G. Luo, "Dynamic Position Estimation Improvement for Sensorless Control of PMSM With ADRC-DPLL Embedded in Current Controller," *25th International Conference on Electrical Machines and Systems (ICEMS)*, Chiang Mai, Thailand, 2022, pp. 1-6.

[4] C. Lascu and G. -D. Andreescu, "PLL Position and Speed Observer With Integrated Current Observer for Sensorless PMSM Drives," in IEEE Transactions on Industrial Electronics, vol. 67, no. 7, pp. 5990-5999, July 2020.

[5] M. Nicola, C. -I. Nicola, A. Vintilă, "Sensorless Control of Multi-Motors PMSM using Back-EMF Sliding Mode Observer," *Electric Vehicles International Conference (EV)*, Bucharest, Romania, 2019, pp. 1-6.

[6] X. Zhang, X. Xie, R. Yao, "Field oriented control for permanent magnet synchronous motor based on DSP experimental platform," *The 27th Chinese Control and Decision Conference (2015 CCDC)*, Qingdao, China, 2015, pp. 1870-1875.

[7] M. F. Elmorshedy, K. M. Kotb, M. K. El-Nemr and A. E. -W. Hassan, "Field-Oriented Control for PMSM in Electric Vehicles Based on 7-level CHB Multilevel Inverter," *23rd International Middle East Power Systems Conference (MEPCON)*, Cairo, Egypt, 2022, pp. 1-7.

[8] F. Chen, J. Liu, S. Feng, J. Yu, Y. Cao, S. Yang, "Research and Simulation of DTC System for PMSM under Inverter Fault," *4th International Conference on Energy, Electrical and Power Engineering (CEEPE)*, Chongqing, China, 2021, pp. 378-382.

[9] B. D. Lemma and S. Pradabane, "Control of PMSM Drive Using Lookup Table Based Compensated Duty Ratio Optimized Direct Torque Control (DTC)," in IEEE Access, vol. 11, pp. 19863-19875, February 2023.

[10] N. Peter *et al*., "Adaptive Field-Oriented Control of Permanent Magnet Synchronous Motor Using Feedfoward Actions," *IEEE International Conference on Advanced Systems and Emergent Technologies (IC_ASET)*, Hammamet, Tunisia, 2023, pp. 1-6.

[11] Z. Huixuan, F. Tao, M. Liu, B. Yuanjun, "Analysis of the Influence of Nonlinear Flux Models on Predictive Current Control in PMSM Drives," *IEEE International Conference on Predictive Control of Electrical Drives and Power Electronics (PRECEDE)*, Jinan, China, 2021, pp. 416-420.

[12] M. Nicola, C.-I. Nicola, C. Ionete, D. Șendrescu, M. Roman, "Improved Performance for PMSM Sensorless Control Based on Robust-Type Controller, ESO-Type Observer, Multiple Neural Networks, and RL-TD3 Agent," in *Sensors*, vol. 23, no. 13, p. 5799, June 2023.

[13] M. S. Reddy, V. S. R. Subrahmanyam, C. S. Prakash, G. V. S. U. Shankar, "Performance analysis of Fuzzy and Neural controller implementation in permanent magnet synchronous motor," *5th International Conference on Intelligent Computing and Control Systems (ICICCS)*, Madurai, India, 2021, pp. 566-574.

[14] M. Kashif and B. Singh, "Modified Active-Power MRAS Based Adaptive Control With Reduced Sensors for PMSM Operated Solar Water Pump," in IEEE Transactions on Energy Conversion, vol. 38, no. 1, pp. 38-52, March 2023.

[15] A. Hezzi, Y. Bensalem, S. Ben Elghali, M. Naceur Abdelkrim, "Sliding Mode Observer based sensorless control of five phase PMSM in electric vehicle," *19th International Conference on Sciences and Techniques of Automatic Control and Computer Engineering (STA)*, Sousse, Tunisia, 2019, pp. 530-535.

[16] Z. Che, H. Yu, S. Mobayen, M. Ali, C. Yang, A. Bartoszewicz, "An Improved Extended State Observer-Based Composite Nonlinear Control for Permanent Magnet Synchronous Motor Speed Regulation Systems," in Energies, vol. 15, no. 15, pp. 1-14, Aug. 2022.

[17] K. Lee, J. Lee, J. Back, Y. I. Lee, "A Robust Emulation of Mechanical Loads Using a Disturbance-Observer," in Energies, vol. 12, no. 12, pp. 1-14, June 2019.

[18] J. Cui, W. Xing, H. Qin, Y. Hua, X. Zhang, X. Liu, "Research on Permanent Magnet Synchronous Motor Control System Based on Adaptive Kalman Filter," in Applied Sciences, vol. 12, no. 10, pp. 1-12, May 2022.

[19] R. Luo, Z. Wang, Y. Sun, "Optimized Luenberger Observer-Based PMSM Sensorless Control by PSO," in Modelling and Simulation in Engineering, vol. 2022, pp. 1-17, August 2022.

[20] M. Asim, A. Verma, M. R. Mahboob, "Load Frequency Control of Multi-Area Power System using Sine-Cosine Algorithm (SCA)," *2nd International Conference on Emerging Frontiers in Electrical and Electronic Technologies (ICEFEET)*, Patna, India, 2022, pp. 1-6.

[21] M. Nicola and C. -I. Nicola, "Improvement of PMSM Control Using Reinforcement Learning Deep Deterministic Policy Gradient Agent," *21st International Symposium on Power Electronics (Ee)*, Novi Sad, Serbia, 2021, pp. 1-6.

[22] *Real-Time Testing – Deploying a Reinforcement Learning Agent for Field-Oriented Control*. Mathworks. [Online]. Available: https://www.mathworks.com/videos/reinforcement-learning-agent-deployment-real-time-testing-on-a-speedgoat-machine-1638925352260.html